Journal of nanoporous Systems

Original Research Paper

Application of SBA-16 nanoporous and its derivatives as drug delivery systems: Mini review

Maryam Razavi Mehr
Department of Education, Faculty of Teacher Education, Farhangian University, Boroujerd, Iran

Article history
Received: 8 November 2025
Revised: 25 December 2025
Accepted: 3 January 2026

*Corresponding Author,
Maryam Razavi Mehr,
Department of Education,
Faculty of Teacher Education,
Farhangian University,
Boroujerd, Iran

Email:
ma.razavimehr@gmail.com

Abstract: SBA-16 (Santa Barbara Amorphous) has a high surface-to-volume ratio due to its villi structure. This unique feature contributes to its thermal and physicochemical stability, making it widely applicable in chromatography, molecular imaging, catalysts, and the pharmaceutical industry. Recently, its lack of molecular toxicity, has attracted the attention of many researchers as a potential drug delivery system. Furthermore, mesoporous silica, particularly SBA-16, has shown a higher drug loading capacity compared to other carriers. Mesoporous silica not only offers a high drug loading capacity, but also enables the control control the rate of drug release rates through functionalizing the inner wall. In this review, I will examine findings from various articles on the use of SBA-16 and its derivatives in drug delivery and pollutant removal applications.

Keywords: SBA-16, Drug delivery, Mesoporous silica nanoparticles, adsorbent.

Introduction

In the pharmaceutical sector, nanotechnology has great potential. With the use of novel drug targeting techniques, medications are now being developed that are more potent and profitable. Knowing that 13% of the vast pharmaceutical industry market is now comprised of the sale of products, such as silicate drug delivery systems [1], makes these consequences more evident. Controlling drug release mechanisms can be quite helpful in managing treatment modalities using medications. Numerous materials have been introduced as drug release systems thus far, including biodegradable polymers, ceramic materials like hydroxyapatite and calcium phosphates, members of the SBA family, and more [2-4].

The regulated and targeted drug delivery approach prevents the drug's toxicity, destruction, and repeated usage. Materials intended to use as drug carriers must good biocompatibility and a high drug-loading capability. To prevent rapid diffusion, the design of these materials must be flawless. Mesoporous materials are employed as drug carriers due to their distinct characteristics, such as a higher surface-to-volume ratio, manageable particle size effect, and biocompatibility and biodegradability. The use of mesoporous silica nanoparticles in medicine has been the subject of increased research in recent years [5–8]. The high porosity of mesoporous silica materials, allows biologically active molecules of varying sizes to settle in the pores of these materials [9]. Additionally, the consistent porosity network of these materials allows for the proper rate of loading and release. Since molecular adsorption in mesoporous materials is a surface phenomenon, the high specific surface area of these materials also leads to increased adsorption of bioactive molecules [10].

Efforts to create various types of silica nanoparticles began at the start of the twenty-first century. New mineral substrates in nanometer dimensions with consistent structures were produced using organic silanes in conjunction with structure-directing agents or modifiers and a solvent mixture of water and alcohol [11]. Silica-based mesoporous Santa Barbara amorphous (SBA) materials have been widely utilized as drug delivery systems. Due to their favorable surface and physicochemical characteristics. These include low toxicity, biocompatibility, biodegradability, and cost-effective production using inexpensive materials. SBA-15 and SBA-16 quickly identified as particularly promising materials in this field. Like other porous materials, the three-dimensional silicate porous materials known as SBA-15 and SBA-16, which contain SiO_2 and surface hydroxyl (OH) groups, are made using non-ionic copolymers as a template and have an amorphous structure [12]. While SBA-16 crystallizes in a cubic crystal structure, SBA-15 does so in a hexagonal one. The three-dimensional cubic shape with open channels, of SBA-16 has drawn more attention due to its Im3m

space group.

The main subset of these materials is SBA-16, which possesses a high surface area, uniform pore size, high pore volume, thermal and chemical stability, hydrophobicity or controllable hydrophilicity, water insolubility, nontoxicity, strong mechanical resistance, and a high concentration of active sites on its surface. It also has a narrow and tunable pore size distribution ranging from 2 to 50 nm, a wall thickness of approximately 3 to 4 nm, and superior mechanical and hydrothermal stability compared to MCM-41 compounds [13]. The mentioned characteristics make these materials ideal for absorption, allowing nanoparticles to evenly distribute across the pores and enhance the resulting mesoporous features. Additionally, loading nanoparticles onto SBA prevents their aggregation and improves the effectiveness of the nanocarrier as a drug delivery mechanism [14]. However, the surfaces of the mesoparticles only contain a limited variety of functional groups primarily silane groups. This limitation restricts the potential applications of these materials for specific target molecules. Several studies have proposed modifications to the active sites of SBA-16 as a solution. These modifications include adding various ligands (such as organic groups, coordination compounds, nanoparticles, and metal oxides) and loading different chemicals onto them. [15, 16].

In this study, I will discuss the research that has been conducted on the use of Nanoporous SBA-16 and its derivatives as drug delivery systems.

Nanoporous SBA-16 and its derivatives as drug carrier systems

Because of its uniform three-dimensional structure and accessible pores, nanoporous SBA-16 performs better as a novel drug carrier. Figure 1 illustrates the overall procedure for making SBA compounds.

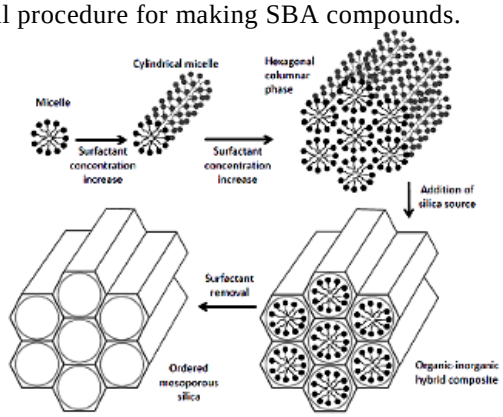

Fig. 1. General synthesis steps of SBA.

Zhao et al. were the first trsearchers that create SBA-type mesoporous materials, which are members of the ceramic family, in 1998. The synthesis of these molecules involves hydrolyzing a silica source, generally tetraethyl orthosilicate, in a two-phase solution. The Pluronic copolymer F127, with a pore size of more than 5 nm, is used to create the cubic structure of SBA-16. In a study conducted by Kim, et al. [17], the aim was to produce SBA-16 with larger pore diameters. They achieved this by using a combination of Pluronic F127 and Pluronic P123 agents, resulting in SBA-16 with pore sizes ranging from 4. 5 to 9. 0 nm. Differences in synthesis temperature, duration, and template composition are responsible for the desired outcomes. Using tetraethyl orthosilicate as a silica source and HCl at low concentrations, Gubin et al. [9] examined the synthesis of SBA-16 with Pluronic F127 in aqueous solution and butanol. The ideal synthesis conditions for SBA-16 yielded a surface area of 886 m^2 g^{-1}, a pore volume of 0. 77 cm^3 g^{-1}, and a pore diameter of 10. 4 nm.

The temozolomide medication was transported via SBA-16 in a 2024 experiment by Soleymani et al. [18]. The drug carrier used in this investigation was the mesostructure of SBA-16. To verify the structure of SBA-16 after production, the physicochemical properties were determined using elemental analysis (EDX), X-ray diffraction (XRD), Fourier transform infrared spectroscopy (FTIR), scanning electron microscopy (SEM), and transmission electron microscopy (TEM). Response surface methodology (RSM), central composite design (CCD), and design of experiments software (DOE) were employed to analyze the impact of effective parameters, such as pH, starting drug concentration, quantity of nanocarrier, temperature, and contact time, on drug loading. The drug release was tested at 37 ^oC in three simulated body environments: neutral, acidic, and alkaline with pH values of 6. 8, 4. 8, and 7. 4, respectively. Measurements were taken at 1, 2, 3, 4, 12, 24, 48, and 72 hours. Data from isotherm and drug loading kinetics experiments revealed that the drug loading process follows the Langmuir isotherm with R^2=0.9964 and the pseudo-second order kinetic model with R^2=0.9992. Additionally, thermodynamic investigations showed that the drug loading process on the SBA-16 nanocarrier is both exothermic and spontaneous. Figure 2 illustrates the analyses conducted, demonstrating the proper preparation of SBA-16. The statistical design of experiments approach was utilized in this study to optimize outcomes. The study concluded that pH had the greatest impact on drug loading, while contact time had the least. The optimal conditions for maximizing drug loading (98.78%) according to the program are a pH of 2, a nanocarrier quantity of 0. 04 g, a drug concentration of 10 mg/L, a temperature of 40 ^oC, and a contact time of 10 minutes.

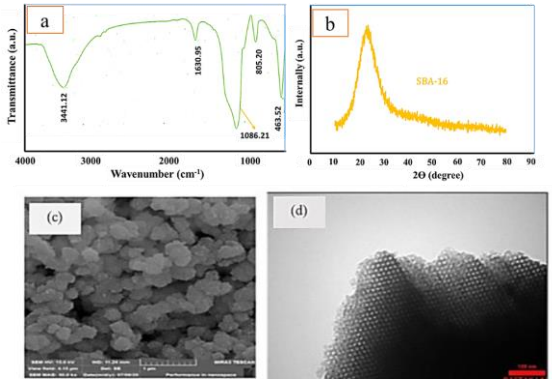

Fig. 2. (a) FTIR spectrum, (b) XRD analysis, (c) SEM and (d) TEM images.

In Figure 3, the drug release graph shows three acidic environments (red graph), an alkaline environment (blue graph), and a neutral environment (green graph). The release rate of temozolomide from the SBA-16 nanocarrier is higher in acidic conditions (pH = 4. 8) than in alkaline and neutral environments (pH = 7. 4 and 6. 8, respectively). After 72 hours, 42% of the drug has been released from the SBA-16 nanocarrier in acidic conditions, 39% in alkaline conditions, and 37. 9% in neutral conditions. Initially, the release of drug molecules adsorbed on the surface of the nanocarrier, is explosive during the first few hours, but then it stabilizes due to the release of drug molecules adsorbed within the nanocarrier's pores.

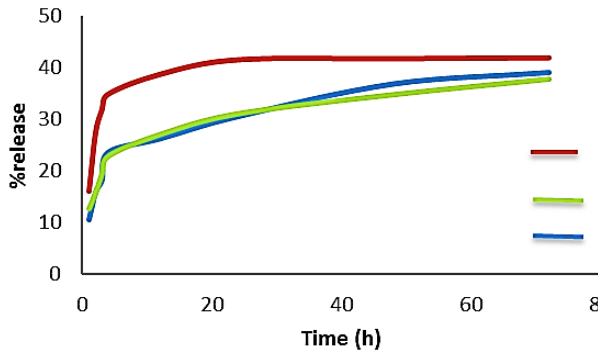

Fig. 3. Temozolamide drug release in three acidic, alkaline, and neutral environments

In a related study, Fikri et al. [19] utilized nanosilica SBA-16 as a carrier for carbamazepine medication. The results indicated that the carbamazepine drug exhibited enhanced adsorption and sustained release when administered optimal conditions.

The medication loading effectiveness under these circumstances was 99. 87%. Furthermore, the experiment demonstrated regulated medicine release. Thermodynamic data showed that the drug loading process is exothermic and spontaneous. The Langmuir isotherm with a regression coefficient of 0.9991 described the adsorption process. The first-order kinetic model with a regression coefficient of 0.9996 described the drug release.

Functionalizing the nanocarrier with functional groups such as $–NH_2$ is currently being explored as a method to enhance efficacy and improve the interaction between the nanocarrier and the drug [20]. To functionalize SBA-16 with $–NH_2$, 3 g of F127 copolymer were dissolved in 144 mL of distilled water and 9 mL of hydrochloric acid. The mixture was stirred at 35 °C until the surfactant was completely dissolved. Then, 9 mL of 1-butanol alcohol were added and the mixture, was stirred for an hour. Next, 13. 2 g of TEOS and 0. 85 mL of 3-aminopropyltrioxysilane were added to the solution. The mixture was stirred on a magnetic stirrer at 100°C for an additional 24 hours. The template was removed using ethanol extraction. The drug Temozolomide, was carried by SBA-16-NH_2 [21]. The results of the BET experiment on mesoporous SBA-16-NH_2 are outlined in Table 4. The data shows that, the specific surface area of SBA-16-NH_2 is 258.64 m^2/g. Furthermore, the average particle diameter and pore volume were 4. 098 nm and 0. 5876 cm^3/g, respectively. This indicates that the produced SBA-16-NH_2 is mesoporous [30]. Thermogravimetric analysis was conducted to determine the thermal stability of the samples, as illustrated in Figure 4. The decrease in mass between room temperature and 200°C is directly related to the amount of absorbed moisture that is released. It is important to note that the presence of amino groups actually decreases the amount of mass lost within this range. The decomposition of the amine ligands occurred thermally at higher temperatures, and it was completed at 800 °C. In samples modified with amine groups, only one major peak was observed at 400 °C. Within the recommended range provided by the software, five factors pH, nanocarrier amount, initial drug concentration, temperature, and contact time—were examined to determine the optimal conditions for maximizing drug loading. The experimental design software suggested pH of 2.73, a nanocarrier dose of 0.045 g, a drug concentration of 10 mg/L, a temperature of 30°C, and a contact time of 10 minutes as the best combination to achieve the highest drug loading of 99.99% with a desirability rating of 1. Following, the commended optimal conditions, the experiments were conducted once more. The data obtained suggest that temozolomide can be effectively delivered using mesoporous SBA-16-NH_2.

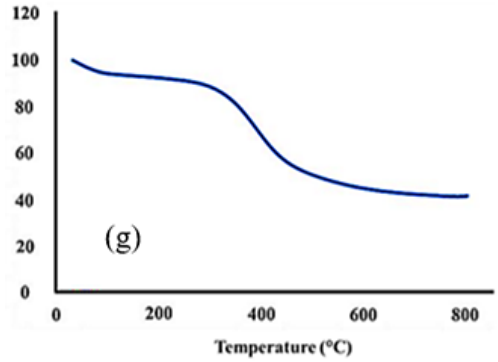

Fig. 4. TGA analysis of SBA-16-NH_2.

Figure 5a displays the FTIR spectrum of SBA-16-NH_2. In Figure 5a, the symmetric stretching vibration of the O-H bond of the Si-OH silanol groups is represented by a wide peak at 3441.12 cm^{-1}. Additionally, the peak at 1630.95 cm^{-1} is related to the stretching and bending motions of the water molecules adsorbed onto the SBA-16 surface. The symmetric and asymmetric Si-O-Si bending, stretching, and bending vibrations are associated with peaks at 463.52 cm^{-1}, 805.20 cm^{-1}, and 1086.21 cm^{-1}, respectively. The data presented above support the conclusion that the manufactured material is a silicate mesoporous [22]. The band observed at 1085.30 cm^{-1} is associated with the asymmetric stretching vibrations of Si-O-Si, while the symmetric stretching vibrations of the Si-O-Si bond are represented by the bands at approximately 797.37 cm^{-1} and 949.10 cm^{-1}. Additionally, the presence of SiO_4 units in the region around 471.94 cm^{-1} indicates tetrahedral silica. The broad band at 16.3414 cm^{-1} is indicative of the O-H stretching vibration mode of silanol groups. In the spectrum of the amine-containing sample, bands associated with C-H stretching vibrations of propyl chains were observed around 2930 cm^{-1}. In the spectrum of the amine-containing sample, the (C-H) ν and (C-H)δ deformation vibrations in methyl groups were observed in the regions of 1463.39 cm^{-1} and 1353 cm^{-1} [23]. Additionally, the XRD study related to mesopore SBA-16-NH_2 revealed a very prominent peak at 2θ = 20-30°. The low-angle X-ray diffraction (XRD) pattern of SBA-16-NH_2 confirms the presence of a well-ordered mesoporous structure with a three-dimensional cubic symmetry of Im3m, which is typical of SBA-16 materials. The reflections from various planes of the cubic mesoporous network are represented by distinct diffraction peaks in the low 2θ range (usually between 0. 8° and 1. 5°). These peaks indicate a mesoporous structure with cubic geometry that is highly organized and coherent. Slight changes in intensity and location of these peaks are observed after functionalization with amino groups (-NH_2), indicating successful grafting of the amino groups onto the pore walls while preserving the original mesoporous structure. The slight decrease in peak intensity is believed to be due to partial filling of the mesopores by the grafted amino groups, which has minimal impact on the diffraction pattern. The low-angle XRD data confirms that SBA-16-NH_2 maintains its three-dimensional cubic Im3m mesoporous structure and the surface functionalization does not cause structural breakdown (Fig. 5c). The scanning electron microscope (SEM) image of the surface of the produced SBA-16 and SBA-16-NH_2 samples is shown in Figure 5d. This micrograph indicates that the synthesized samples of SBA-16 and SBA-16-NH_2 have a uniform, spherical shape. Moreover, the pore size ranges from 2 to 50 nm, demonstrating that the material created is mesoporous [24]. A TEM image of the SBA-16-NH_2 mesostructured material at a magnification of 100 nm is shown in Fig. 5e. This image illustrates a highly organized cage-like arrangement of mesopores. The adsorption-desorption isotherm plot of SBA-16-NH_2 is depicted in Fig 5f. In this nanocomposite, the adsorption curve does not align with the desorption curve, forming a hysteresis loop characteristic of a type IV isotherm. A material is considered to have 100% mesoporous when its isotherm graph displays a hysteresis loop and the shape of the pores can be determined by analyzing the hysteresis loop and the adsorption-desorption isotherm plot. According to the diagram, the hysteresis loop falls under the H1 type, indicating that the pores have a cylindrical shape [25].

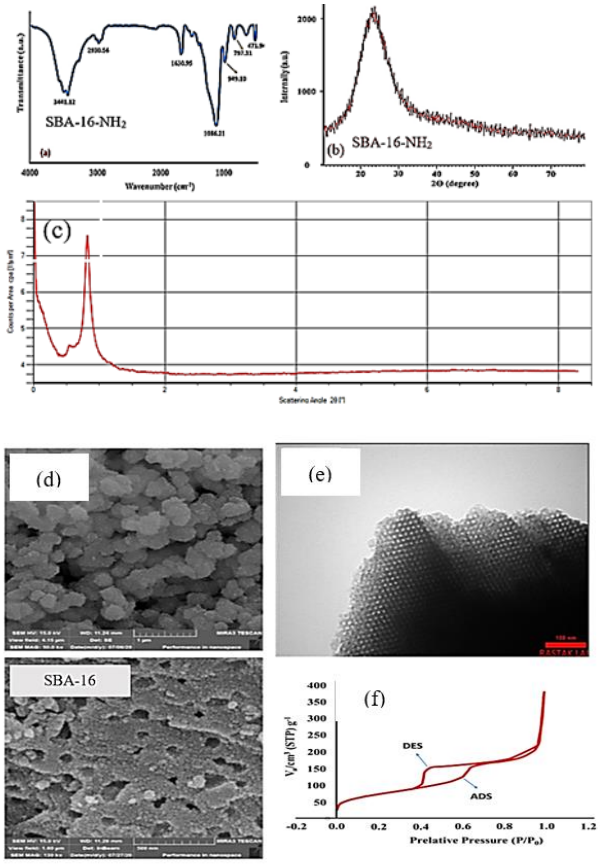

Fig 5. (a) FTIR spectrum, (b) XRD analysis, (c) low angle XRD pattern, (d) SEM image, (e) TEM image, (f) adsorption-desorption isotherm diagram of SBA-16-NH_2

According to the BET study, the specific surface area of SBA-16-NH_2 is 258.64 m^2/g. Additionally, the average particle size and pore volume were determined to be 4.098 nm and 0.5876 cm^3/g, respectively. Therefore, it can be concluded that the produced SBA-16-NH_2 is mesoporous.

One downside of nanoparticles is their tendency to become isolated from the liquid phase. The centrifuge is commonly used to separate nanoparticles from the liquid phase, but it is not always very effective. Using magnetic particles in the nanocomposite structure and then easily separating them with a magnet is one helpful technique for isolating nanoparticles from the solvent. The extraction of ferromagnetic and paramagnetic particles from mixtures is achieved through magnetic separation in various industries. One of the key advantages of this method is that it is a clean, chemical-free process that does not harm threat to the environment. Magnetic separators are highly efficient in separating magnetic particles from non-magnetic materials, making them ideal for applications requiring high purity levels. Magnetic separation can recover a wide range of magnetic materials, from ferromagnetic to paramagnetic particles.

In another study, Fe_3O_4 magnetic nanoparticles were loaded on SBA-16/NH_2 using the in situ method [26], creating the Fe_3O_4/NH_2-SBA-16 mesostructure as nanocarriers for loading and releasing phenobarbital medication. In this study, the Stopper method [27, 28] was employed to magnetize Fe_3O_4. Initially, 0.994 g of $FeCl_2$. $4H_2O$ and 2.702 g of $FeCl_3$. $6H_2O$ were dissolved in 10 mL of distilled water. The mixture was then agitated in a three-hole beaker under a nitrogen environment. Subsequently, 20 mL of ammonia was added to the flask while stirring (pH between 9). A magnet was used to separate the resulting precipitate (black in color) from the solvent, and it was then rinsed with 96% ethanol. The Fe_3O_4 nanoparticles were dried for 18 hours in a 65 °C oven. The following equation represents the overall response of the Fe_3O_4 preparation. For the synthesis of Fe_3O_4/NH_2-SBA-16, 60 mg of Fe_3O_4 was dispersed in 20 mL of ethanol, followed by the addition of 0. 2 g of SBA-16/NH_2. The mixture was stirred at room temperature for 8 hours. The produced nanocomposite was then dried at ambient temperature after being separated from the solvent using a magnet.

The FTIR and XRD spectra in Figures 6 and 7 demonstrate the synthesis of the SBA-16-NH_2 nanostructure magnetized by Fe_3O_4 effectively.

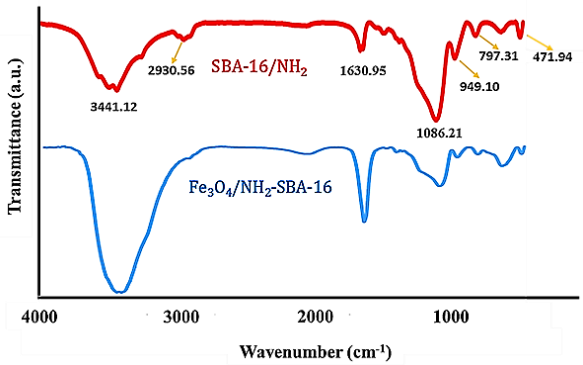

Fig. 6. FTIR peaks of SBA-16/NH_2 and Fe_3O_4/NH_2-SBA-16 in the region of 4000–400 cm^{-1}.

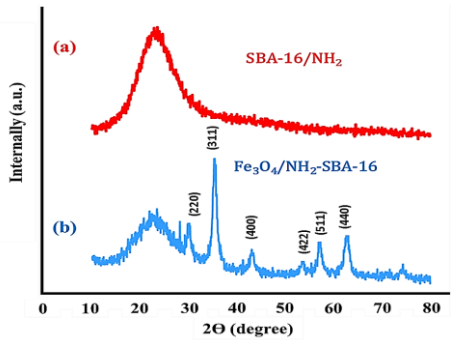

Fig. 7. XRD patterns of (a) SBA-16/NH_2 and (b) Fe_3O_4/NH_2-SBA-16 nanoparticles.

The successful placement of Fe_3O_4 particles on the SBA-16/NH_2 mesostructure (black spots) is also visible in scanning electron microscope images (TEM) of the Fe_3O_4/NH_2-SBA-16 nanocomposite (Fig. 8). The TEM images clearly show that the morphology of SBA-16/NH_2 is maintained after the addition of Fe_3O_4, with no noticeable modifications [29].

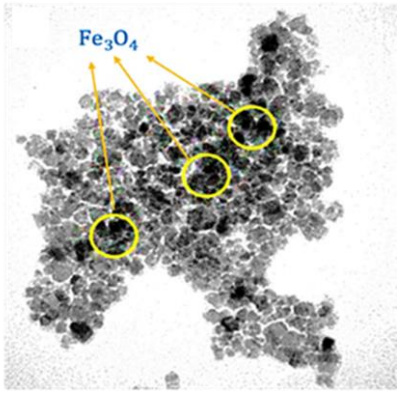

Fig. 8. TEM micrograph of Fe_3O_4/NH_2-SBA-16.

The Ag/ZnO/SBA-16 composite was created and utilized as a phenobarbital drug delivery system in a study conducted by Fikri *et al*. in 2024. Because of its simple fabrication process, distinct morphology, spacious pore size, and, especially the interconnected three-dimensional

pore structure that enhances mass transfer, Ag/ZnO/SBA-16 mesoporous material was used in this study as a carrier for phenobarbital drug. After being identified using a variety of methods (XRD, SEM, TEM, etc.), the newly produced nanocomposite was used in research on drug loading and release. The EDX examination of the mesostructure of SBA-16 (Fig. 9a) reveals that silicon has the highest peak compared to other elements, supporting the conclusion that SBA-16 is a silicate material. The presence of Zn and Ag peaks in Figure 9b confirms that the Ag/ZnO/SBA-16 nanocomposite has been properly manufactured. The peak associated with Si is still the highest, demonstrating that this mesopore has retained its silicate structure in addition to the accurate structure of the manufactured nanocomposite.

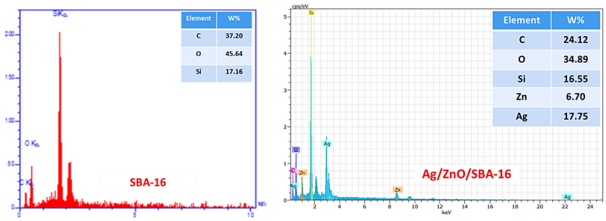

Fig. 9. EDX analysis of (a) SBA-16 and (b) Ag/ZnO/SBA-16.

The adsorption/desorption isotherm and BJH curve of the Ag/ZnO/SBA-16 nanocarrier are shown in Figures 10a and 10b, respectively. As shown in Figure 10a, this nanocomposite displays a type IV (a) isotherm (according to IUPAC terminology) and hysteresis in the absorption/desorption mechanism [30]. A compound is considered entirely mesoporous if its isotherm plot shows a hysteresis loop. The shape of the pores can determine by analyzing the hysteresis loop and the adsorption-desorption isotherm plot. In this case, the hysteresis loop is of the H1 type, indicating that the pores are cylindrical in shape [31, 32]. The BJH curve of the nanocomposite between 1 and 100 nm is displayed in Figure 8b. This curve can be used to determine the size distribution of the holes. The maximum distribution of pores in the manufactured nanocomposite falls between 1 and 10 nm. Additionally, the BET study of the Ag/ZnO/SBA-16 nanocomposite revealed a specific surface area of 276.87 m^2/g. Additionally, the average particle diameter and pore volume were found to be 10.90 nm and 0.5378 cm^3/g, respectively. Therefore, the synthesized nanocomposite can be said to be classified as mesoporous. According to the IUPAC classification, materials with pore sizes between 2 and 50 nm are considered mesoporous, indicating that nanomaterials, a subset of nanostructured materials, contain nanometer-scale pores [33]. This type of material, with a significantly large internal surface area, is highly effective at absorbing and interacting with atoms, molecules, and ions. The BET analysis results indicate that Ag/ZnO/SBA-16 processes a nanoscale structure due to the presence of nanoscale pores.

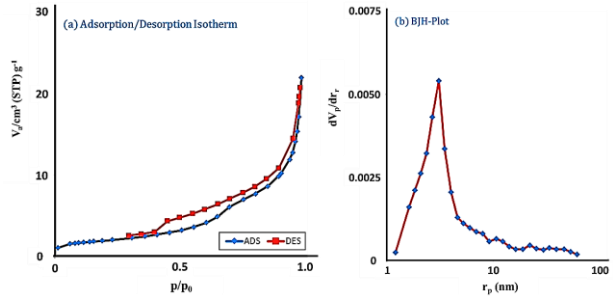

Fig 10. (a)Adsorption/desorption analysis and (b) BJH-plot of Ag/ZnO/SBA-16 nanocomposite.

The percentage of medication loaded onto the nanocomposite was significantly impacted by five factors. The effects of temperature, contact time, pH, initial drug concentration, and composite dosage were studied using the RSM approach.

The Ag/ZnO/SBA-16 nanocomposite, showed the highest amount of drug loading at pH = 2.82. The results indicated there is an inverse relationship between pH and loading percentage. At a low pH (lower than pH_{pzc}=7.9), the nanocomposite surface becomes more positive as H^+ ions are adsorbed onto the nanocomposite sites. This leads to the protonation of the amine group in the phenobarbital drug, resulting in an increased drug loading rate. However, at high pH (greater than pH_{pzc}), the drug loading decreases due to repulsion between the nanocarrier surface and the drug which reduces the concentration of OH^- ions on the surface [34]. The surface charge is zero at the point of zero charge (pH_{pzc}) because the positive and negative charges are equal at that point [35]. The pH of a solution was created by dissolving 0. 01 g of the PHB drug in 15 mL of distilled water. The pH was initially adjusted to a range of 2 to 12 in order to determine the pH_{pzc}. The solution was then placed on a magnetic stirrer for an hour. The final pH was measured and pH_{pzc} was found to be 7.9 according to Figure 11. If there were no surface charge, the pH value would be different, and the graph would appear green instead of red.

pH_i	2.00	3.00	4.00	5.00	6.00	7.00	8.00	9.00	10.00	11.00	12.00
pH_f	2.11	6.67	6.70	6.75	6.83	7.25	7.95	8.46	9.76	10.97	11.96

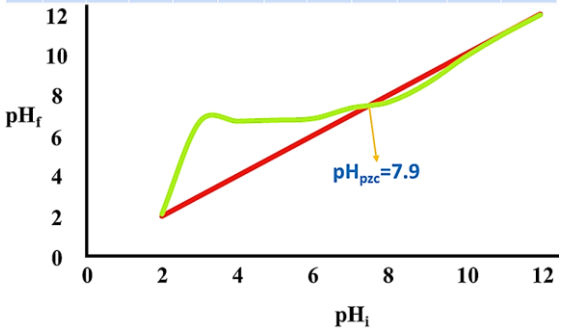

Fig. 11. pH_{PZC} of Ag/ZnO/SBA-16 nanocomposite.

The study investigated the impact of the dose of Ag/ZnO/SBA-16 nanocomposite on the percentage of EE, with beneficial results (p-value < 0. 05). It was observed that the quantity of medication loaded increased as the amount of nanocomposite increased. This is because increasing the amount of nanocarrier provides more active sites and a larger surface area for drug molecules to load onto. The maximum amount of nanocomposite that can be loaded with drugs is 0. 04 grams [20].

Furthermore, the drug loading percentage is inversely proportional to the starting drug concentration. The optimal starting drug concentration for this investigation was found to be 10 ppm. The loading rate decreases as the initial concentration increases [36]. This is because, at higher concentrations, all the active sites of the drug carrier are filled with drug molecules. Temperature is another variable that can influence the loading of phenobarbital medicines onto the Ag/ZnO/SBA-16 nanocomposite. The process of loading drugs onto the nanocarrier was studied at five temperatures 30, 40, 50, 60, and 70°C. According to the findings, the amount of medicine loaded onto the nanocarrier decreases as the temperature increases. Changes in Gibbs free energy are responsible for the decrease in loading. The enthalpy change is negative (exothermic) and the entropy change is positive during the adsorption process. With the decrease in temperature, Gibbs free energy becomes negative, causing the absorption process to occur spontaneously. This is illustrated in Table 1, based on the equation $\Delta G = \Delta H - T\Delta S$ [37].

Table 8. Thermodynamic parameters for the adsorption of PHB drug onto Ag/ZnO/SBA-16 at different temperatures.

Temp. (K)	$\ln K_c$	ΔH° ($Kj.mol^{-1}$)	ΔS° ($Kj.mol^{-1}$)	ΔG° ($Kj.mol^{-1}$)
303	4.45			-11.24
313	3.91			-10.86
323	3.88	-22.85	-0.038	-10.47
333	3.63			-10.09
343	3.35			-9.71

The drug loading capacity is directly proportional to the contact period necessary to achieve stable absorption. The findings demonstrate that the loading rate increases quickly for the first 13 minutes as a result of an increase in the available surface area of mesoporous silica particles. This indicates that the medicine molecules have access to a significant number of active sites on the nanocomposite during the first few minutes, resulting in higher drug loading [38]. The drug release experiment graphs for three aqueous environments (green curve), an acidic environment (blue curve), and an alkaline environment (red curve) are shown in Figure 12. In 2011, Zeng *et al*. published a theoretical kinetic model for drug release by silica nanoparticles [39].

The premise of this model is that drug release occurs explosively during the early hours and then slowly and steadily, depending on the release of drug molecules located inside the pores of silica nanoparticles. According to the study, 10% of the total drug was released from the nanoparticles during the first four hours, indicating a rapid release. Drug absorption at the particle surface (surface loading) of nanoparticles may explain the quick release of drugs from nanoparticles. The drug's presence on the surface of the nanoparticles could account for its early, rapid release. Drug molecules adsorbed on the surface of the nanoparticles are released more quickly than embedded medication. However, it was discovered that the drug release was still occurring [40].

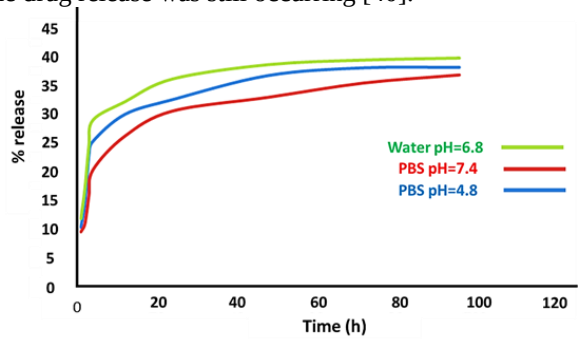

Fig. 12. *In vitro* release of PHB by Ag/ZnO/SBA-16 nanocomposite.

Ag particles are effective against a wide variety of microbial species because they release Ag ions [41]. In reality, Ag ions are a powerful antibacterial agents multifaceted attack against susceptible and resistant bacteria [42]. However, the oxidation of Ag ions causes them to aggregate, resulting in the loss of their bioactivities [43, 44]. Using an appropriate substrate could be an effective strategy decrease prolonged bioactivities in this situation. In order to accomplish this, the substrate must protect Ag nanoparticles to inhibit the rapid release of ions. Ag/SBA-16 is considered a perfect support for loading and transporting Ag nanoparticles over long periods due to its controlled ion release [45]. However, Ag/SBA-16 is expected to maintain bioactivities because of its higher loaded Ag and more complex pore structure [46]. In contrast, SBA-16 lacks biological activity due to its biodegradability. Additionally, its porosity may support the growth of simpler microorganisms, resulting in no antibacterial activity at any stage. The highly loaded Ag nanoparticles in Ag/SBA-16 are predicted to demonstrate prolonged and efficient bioactivities thanks to their controlled release at the appropriate dose. This characteristic persists until a sufficient ion dose is present in the bulk tubes [47]. In addition, four zero-order (ZO), pseudo-first-order

(PFO), pseudo-second-order (PSO), and Higuchi model (HIG) were examined to determine the optimal kinetic model for the release of the PHB drug in three aqueous, acidic and alkaline environments. According to the Higuchi kinetic model (R^2= 0.9969, 0.9991, and 0.9992 for aqueous, acidic, and alkaline environments, respectively) and drug loading, the results demonstrate that drug release follows this model.

Conclusions

The focus of the present stusy was on the synthesis of SBA-16 and its derivatives as drug delivery systems. Various techniques such as Infrared spectroscopy (FTIR), X-ray diffraction (XRD), scanning electron microscopy (SEM), transmission electron microscopy (TEM), and nitrogen sorption analysis were utilized to analyze the mesoporous structure. Furthermore, the release and loading of drugs from SBA-16 and its derivatives were investigated. The release features were evaluated, and the percentage of encapsulation loading efficiency was analyzed using Design of Experiment software. The results indicate that the highest adsorption rate can be achieved by optimizing the effective variables involved in drug loading. The study identified pH as the variable with the greatest impact and contact time as the variable with the least impact on the effectiveness of drug encapsulation onto nanocomposites.

Studies on drug release reveal that the drug is released rapidly during the initial hours, followed by a controlled release over time. The thermodynamic and kinetic data support the conclusion that physical adsorption causes the drug to spontaneously and exothermically adsorb onto the nanocarrier. Additionally, when comparing different models, the pseudo-second-order model better captures the adsorption and release of medications. The results obtained suggest that mesoporous SBA-16 and its family are ideal drug delivery systems for temozolomide.

Acknowledgements

The author expresses their appreciation to post-graduate office of Farhangian University for financial support of this work.

References

[1] Taylor, K. M., Kim, J. S., Rieter, W. J., An, H., Lin, W., Lin, W., Mesoporous Silica Nanospheres as Highly Efficient MRI Contrast Agents. ***J. Am. Chem. Soc.,*** **2008**, 130, 2154. https://doi.org/10.1021/ja710193c.

[2] Shin, Y., Chang, J. H., Liu, J. R., Williford, R., Shin, Y. K., Exarhos, G. J., Hybrid nanogels for sustainable positive thermosensitive drug release. ***J. controlled release,*** **2001**, 73, 1. doi: 10.1016/s0168-3659(01)00247-4.

[3] Han, Y. J., Yu, Z. T., Zhou, L., Hydroxyapatite/titania composite bioactivity coating processed by the sol–gel method. ***Biomed. Mate.,*** **2008**, 3, 044109. doi: 10.1088/1748-6041/3/4/044109.

[4] Vallet-Reg, M., Gonzalez-Calbet, J. M., Calcium Phosphates as Substitution of Bone Tissues. ***Prog. solid state Chem.,*** **2004**, 32, 1, http://dx.doi.org/10.1016/j.progsolidstchem.2004.07.001.

[5] Talib, M., Abd Alkadir, A., Synthesis and characterization of mesoporous materials as a carrier and release of prednisolone in drug delivery system. ***Journal of Drug Delivery Sci. Technol.,*** **2019**, 53, 101176. https://doi.org/10.1016/j.jddst.2019.101176.

[6] Morales, V., Martin, A., Ortiz-Bustos, J.; Sanz, R., Effect of the dual incorporation of fullerene and polyethyleneimine moieties into SBA-15 materials as platforms for drug delivery. ***J. Mater. Sci.,*** **2019**, 54, 11635. doi: 10.1007/s10853-019-03708-0.

[7] Trzeciak, K., Chotera-Ouda, A., Bak-Sypien, I. I., Potrzebowski, M. J., Mesoporous Silica Particles as Drug Delivery Systems—The State of the Art in Loading Methods and the Recent Progress in Analytical Techniques for Monitoring These Processes. ***Pharmaceutics,*** **2021**, 13, 950, doi: 10.3390/pharmaceutics13070950.

[8] Fekri, M. H., Soleymani, S., Razavi Mehr, M., Akbari-adergani, B., Synthesis and characterization of mesoporous ZnO/SBA-16 nanocomposite: Its efficiency as drug delivery system. ***J. Non-Cryst. Solids,*** **2022**, 591, 121512. https://doi.org/10.1016/j.jnoncrysol.2022.121512.

[9] Prabha, S., Durgalakshmi, D., Rajendran, S., Lichtfouse, E., Plant-derived silica nanoparticles and composites for biosensors, bioimaging, drug delivery and supercapacitors: a review. ***Environmental chemistry letters,*** **2021**, 19, 1667-1691. https://doi.org/10.1007/s10311-020-01123-5

[10] Wang, S., Ordered mesoporous materials for drug delivery. ***Microporous mesoporous mater.,*** **2009**, 117, 1, https://doi.org/10.1016/j.micromeso.2008.07.002.

[11] Morey, M., Davidson, A., Eckert, H., Stucky, G., Silica-Based, Cubic Mesostructures: Synthesis, Characterization and Relevance for Catalysis. ***Chem. Mater.,*** **1996**, 8, 486. https://doi.org/10.1021/cm950397j.

[12] Yu, B., Shi, R., Chen, X., Zhang, Y., Hu, J., Khan, S., Gelatin-coated indomethacin drug-loaded SBA-16 silica-based composites: pH-responsive slow-release performance. ***Inorganic Chemistry Communications.,*** **2023**, 150, 110469. https://doi.org/10.1016/j.inoche.2023.110469.

[13] Costa, J. A. S., de Jesus, R. A., Santos, D. O., Neris, J. B., Figueiredo, R. T., Paranhos, C. M, Synthesis, functionalization, and environmental application of silica-based mesoporous materials of the M41S and SBA-n families: A review. ***Journal of Environmental Chemical Engineering,*** **2021**, 9, 105259. https://doi.org/10.1016/j.jece.2021.105259.

[14] Ezzeddine, Z. Batonneau-Gener, I. Pouilloux, Y., Zinc Removal from Water via EDTA-Modified Mesoporous SBA-16 and SBA-15. ***Toxics***, **2023**, 11, 205. https://doi.org/10.3390/toxics11030205.

[15] Wang, X., Jia, J., Zhao, L., Sun, T., Chemisorption of hydrogen sulphide on zinc oxide modified aluminum-substituted SBA-15. ***Appl. Surf. Sci.,*** **2008**, 254, 5445. https://doi.org/10.1016/j.apsusc.2008.02.086.

[16] Hu, Y., Zhi, Z., Zhao, Q., Wua, C., Zhao, P., Jiang, H., Jiang, T., Wang, S., 3D cubic mesoporous silica microsphere as a carrier for poorly soluble drug carvedilol. ***Microporous Mesoporous Mater.,*** **2012**, 147, 94. doi: 10.1016/j.micromeso.2011.06.001.

[17] Kim, T. W., Ryoo, R., Kruk, M., Gierszal, K. P., Jaroniec, M., Kamiya, S., Terasaki, O., Tailoring the pore structure of SBA-16 silica molecular sieve through the use of copolymer blends and control of synthesis temperature and time. ***The Journal of Physical Chemistry B,*** **2004**, 108(31), 11480-11489. doi:10.1021/jp048582k.

[18] Soleymani, S., Razavimehr,, M., Fekri, M. H., Synthesis and identification of nanoceramic SBA-16 by green method and its application as temozolamide drug delivery system. ***Nanomeghyas,*** **2025**, 4(11), 86-105.

[19] Fekri, M. H., Razavi Mehr, M., Saki, F., Soleymani, S., Preparation and Optimization of Effective Parameters for the Controlled Release of Carbamazepine by Nanosilica SBA-16 as a Drug Carrier. ***J. Mazandaran Univ. Med. Sci.,*** **2024**, 34(237), 14-29.

[20] Soleymani, S., Razavi Mehr, M., Fekri, M. H., Saki, F., Modification of SBA-16 surface by-NH_2 group and its application as adsorbent, ***Chemical Papers,*** **2023,** 77(9), 5129-5141. doi: 10.1007/s11696-023-02849-6.

[21] Soleymani, S., Raavi Mehr, M., Targeted drug delivery of temozolamide to cancer cells using SBA-16 modified mesoporous nanostructure. ***Journal of Nanoporous Systems,*** **2025**, 1(2), 105-122. doi: 10.66437/JNS-2507-1011.1.2.4.

[22] Naghiloo, M., et al. "Functionalization of SBA-16 silica particles for ibuprofen delivery. ***Journal of Sol-Gel Science and Technology,*** **2015,** 74, 537-543. https://doi.org/10.1007/s10971-015-3631-6.

[23] Goscianska, J., Olejnik, A., Nowak, I., APTES-functionalized mesoporous silica as a vehicle for antipyrine–adsorption and release studies, ***Colloids and Surfaces A: Physicochemical and Engineering Aspects,*** **2017,** 533, 187-196. https://doi.org/10.1016/j.colsurfa.2017.07.043.

[24] Feliczak-Guzik, A., Jadach, B., Piotrowska, H., Murias, M., Lulek, J., Nowak, I., Synthesis and characterization of SBA-16 type mesoporous materials containing amine groups. ***Microporous and Mesoporous Materials,*** **2016,** 220, 231-238. https://doi.org/10.1016/j.micromeso.2015.09.006.

[25] Thommes, M., Kaneko, K., Neimark, A. V., Olivier, J. P., Rodriguez-Reinoso, F., Rouquerol, J., & Sing, K. S. W. Physisorption of gases, with special reference to the evaluation of surface area and pore size distribution (IUPAC Technical Report). ***Pure and Applied Chemistry***, **2015**, *87*(9-10), 1051–1069. https://doi.org/10.1515/pac-2014-1117

[26] Fekri, M. H., Razavi Mehr, M., Soleymani, S., Fe_3O_4/SBA-16-NH_2 Nanocomposites: Synthesis, Characterization and Applications as a Phenobarbital Drug Release Systems. ***Phys. Chem. Res.,*** **2025**, 13 (4), 797-816. https://doi.org/10.22036/pcr.2025.538792.2715.

[27] Girginova, P. L., Daniel-da-Silva, A. L., Lopes, C. B., Figueira, P., Otero, M.; Amaral, V. S., Pereira, E., Trindade, T. J., Silica Coated Magnetite Particles for Magnetic Removal of Hg^{2+} from Water. ***Colloid Interface Sci.,*** **2010**, 345, 234-240 doi: 10.1016/j.jcis.2010.01.087.

[28] Fekri, M. H., Tousi, F., Heydari, R., Razavi Mehr, M., Rashidipour, M., Synthesis of Magnetic Novel Hybrid Nanocomposite (Fe_3O_4@SiO_2/Activated carbon (by a Green method and Evaluation of Its Antibacterial Potential. ***Iran. J. Chem. Chem. Eng.,*** **2022**, 41, 767-776. doi: 10.30492/ijcce.2021.128507.4164.

[29] Sayyadi, K., Mohammadi, P., Abaszadeh, M., Sheibani, H., Au Nanoparticles Immobilized in Fe_3O_4/SBA-16 Functionalized Melamine-α-Chloroacetic

Acid as a Recoverable Nanocatalyst for Reduction of Dye Pollutants in Water. ***Chemistry Select,*** **2019**, 4, 7609-7615. doi: 10.1002/slct.201901421.

[30] Zhao, D., Huo, Q., Feng, J., Chmelka, B. F., Stucky, G. D., Nonionic Triblock and Star Diblock Copolymer and Oligomeric Surfactant Syntheses of Highly Ordered, Hydrothermally Stable, Mesoporous Silica Structures. ***J. Am. Chem. Soc.,*** **1998**, 120, 6024. https://doi.org/10.1021/ja974025i.

[31] Kim, T. W., Ryoo, R., Gierszal, K. P., Jaroniec, M., Solovyov, L. A., Sakamoto, Y., Terasaki, O., Characterization of mesoporous carbons synthesized with SBA-16 silica template. ***Journal of Materials Chemistry,*** **2005**, 15, 1560-1571. https://doi.org/10.1039/B417804A.

[32] Wang, X., Mei, J., Zhao, Z., Chen, Z., Zheng, P., Fu, J., Li, H., Fan, J., Duan, A., Xu, C., Controllable Synthesis of Spherical Al-SBA-16 Mesoporous Materials with Different Crystal Sizes and Its High Isomerization Performance for Hydrodesulfurization of Dibenzothiophene and 4,6-Dimethyldibenzothiophene. ***Ind. Eng. Chem. Res.,*** **2018**, 57, 2498. https://doi.org/10.1021/acs.iecr.8b00109.

[33] Banafti, S., Jahanshahi, M., Peyravi, M., Khalili, S., Controllable release activity of antibacterial Ag/SBA-16 cage-like synthesized by one-pot method. ***Microporous and Mesoporous Mater.,*** **2020**, 299, 110107. https://doi.org/10.1016/j.micromeso.2020.110107.

[34] Afrashteh, S., Nouri, N., Banihashem, P., Hoseinpour Kasgari, A., Valipour, P., Binaeian, E., Methotrexate drug uptake through dimethyl ethylenediamine post-modified metal–organic framework as a carrier: optimization using RSM. ***Journal of Porous Materials,*** **2023**, 3, 1625-1641. https://doi.org/10.1007/s10934-023-01441-3.

[35] Bakatula, E. N., Richard, D., Neculita, C. M., Zagury, G. J., Determination of point of zero charge of natural organic materials. ***Environ. Sci. Pollut. Res. Int.,*** **2018**, 2, 7823. doi: 10.1007/s11356-017-1115-7.

[36] Fekri, M. H., Saki, F., Razavi-mehr, M., Soleymani, S., Preparation of SBA-16 silicate nanoabsorbent by green method from reed plant stem, using it to remove Phenolphthalein pollutant and investigating effective factors by RSM method. ***Applied Chemistry,*** **2023**, 271-288. https://doi.org/10.22075/chem.2023.29594.2141.

[37] Fekri, M. H., Mohamareh, S. I., Hosseini, M., Mehr, M. R., Green synthesis of activated carbon/Fe_3O_4 nanocomposite from flaxseed and its application as adsorbent and antibacterial agent. ***Chemical Papers,*** **2022**, 76, 6767-6782. https://doi.org/10.1007/s11696-022-02278-x.

[38] Fard, N. T., Panahi, H. A., Banadaki, M. D., Moniri, E., Soltani, E. R., Surface modification of graphene oxide by functionalized dendritic polyesters based on phthalic acid and pentaerythritol as a novel nanoplatform for sustained drug delivery: Statistical optimization using response surface methodology and release kinetics modelling. ***Materials Today Communications,*** **2023**, 36, 106476, https://doi.org/10.1016/j.mtcomm.2023.106476.

[39] Zeng, L., An, L., Wu, X., Modeling Drug-Carrier Interaction in the Drug Release from Nanocarrier. ***Drug Delivery,*** **2011,** 2011. https://doi.org/10.1155/2011/370308.

[40] Sharma, H., Kumar, K., Choudhary, C., Mishra, P. K., Vaidya, B., Development and characterization of metal oxide nanoparticles for the delivery of anticancer drug. ***Artificial cells, nanomedicine, and biotechnology,*** **2016**, 44, 672-679. https://doi.org/10.3109/21691401.2014.978980.

[41] Ghandour, W., Hubbard, J. A., Deistung, J., Hughes, M. N., Poole, R. K., The uptake of silver ions by Escherichia coli K12: toxic effects and interaction with copper ions. ***Applied microbiology and biotechnology,*** **1988**, 28, 559-565. https://doi.org/10.1007/BF00250412.

[42] Jones, S. A., Bowler, P. G., Walker, M., Parsons, D., Controlling wound bioburden with a novel silver-containing Hydrofiber® dressing. ***Wound repair and regeneration,*** **2004**, 12, 288-294. https://doi.org/10.1111/j.1067-1927.2004.012304.x.

[43] Lok, C. N., Ho, C. M., Chen, R., He, Q. Y., Yu, W. Y., Sun, H., Che, C. M., Silver nanoparticles: partial oxidation and antibacterial activities. ***JBIC Journal of Biological Inorganic Chemistry,*** **2007**, 12, 527-534. https://doi.org/10.1007/s00775-007-0208-z.

[44] Pal, S., Tak, Y. K., Song, J. M., Does the antibacterial activity of silver nanoparticles depend on the shape of the nanoparticle? A study of the gram-negative bacterium Escherichia coli. ***Applied and environmental microbiology,*** **2007**, 73, 1712-1720. https://doi.org/10.1128/AEM.02218-06.

[45] Zhang, X., Qu, Z., Li, X., Zhao, Q., Zhang, X., Quan, X., In-situ synthesis of Ag/SBA-15 nanocomposites by the “pH-adjusting” method. ***Materials letters,*** **2011**, 65, 1892-1895. https://doi.org/10.1016/j.matlet.2011.03.072.

[46] Ouargli, R., Hamacha, R., Benharrats, N., Boos, A., Bengueddach, A., β-diketone functionalized SBA-15 and

SBA-16 for rapid liquid–solid extraction of copper. ***Journal of Porous Materials,*** **2015**, 22, 511-520. https://doi.org/10.1007/s10934-015-9921-0.

[47] de Oliveira Lima, A. M., Fragal, E. H., Caldas, B. S., Nakamura, T. U., Rubia, A. F., Silva, R., Functional mesoporous silica decorated with Ag nanoparticles as chemo-photothermal agents. ***Microporous and Mesoporous Materials,*** **2022**, 341, 112097. https://doi.org/10.1016/j.micromeso.2022.112097.